Letter

Molecular analysis of SMARD1 patient-derived cells demonstrates that nonsense-mediated mRNA decay is impaired

INTRODUCTION

Biallelic mutations in the immunoglobulin μ-binding protein 2 (IGHMBP2) gene lead to motor neuron (MN) degeneration in the brain stem and anterior horns of the spinal cord, causing fatal spinal muscular atrophy with respiratory distress type I (SMARD1). Patients exhibit a certain degree of phenotypic variability that has not been explained.[1] No effective therapy is currently available, and understanding the function of IGHMBP2 is crucial for identifying specific disease targets.

IGHMBP2 is a DNA/RNA helicase protein involved in different cellular processes, but its precise function is unknown. IGHMBP2 exhibits similarities to the human regulator of nonsense transcripts homolog UPF1,[2] which is part of the core complex required for nonsense-mediated mRNA decay (NMD), a translation-dependent RNA degradation pathway implicated in different subtypes of amyotrophic lateral sclerosis (ALS).[3]

We analysed fibroblasts, induced pluripotent stem cells (iPSCs), and their derived MNs from eight patients with SMARD1 carrying different IGHMBP2 mutations. All cell types exhibited a marked deficiency in IGHMBP2 protein but not mRNA. We further demonstrated that the IGHMBP2 transcript is regulated by the NMD pathway, which resulted inhibited in SMARD1 condition.

RESULTS

Our eight SMARD1 patients are summarised in online supplemental table 1. The identified mutations included four missense and four nonsense mutations, three point deletions, one inversion and one insertion mutation (figure 1A). We collected peripheral blood mononuclear cells and/or fibroblasts from the patients and three unaffected subjects (online supplemental table 2). We successfully reprogrammed iPSCs from four patients (online supplemental figure 1A) and differentiated them into MNs (online supplemental figure 1B) that exhibited pathological features of increased apoptosis and decreased axon length (online supplemental figure 1C,D).

Western blot analysis of MNs, fibroblasts and iPSCs from patients and controls (online supplemental figure 2) showed three migration bands specific for IGHMBP2 (~110 kDa,~75 kDa and ~55 kDa). Online supplemental figure 3 summarises the data regarding protein isoforms. Only the ~110 kDa band corresponded to the full-length and functioning IGHMPB2 protein[4]; it was significantly reduced in all SMARD1 samples (figure 1B; online supplemental figure 2) and nearly absent in cell lines with nonsense mutations. Immunofluorescence confirmed the western blot data in MNs (figure 1C) and iPSCs (online supplemental figure 4), with no difference in localisation. Interestingly, our analysis suggested that the reduction in IGHMBP2 was not the result of decreased mRNA (figure 1C; online supplemental figure 5A).

To determine whether the upregulation of IGHMBP2 mRNA in SMARD1 was attributable to impaired mRNA turnover, we evaluated the efficacy of IGHMBP2 mRNA decay after transcriptional inhibition in iPSCs. The ratio of mRNA before and after actinomycin D treatment was increased in SMARD1 iPSCs (online supplemental figure 5B), suggesting an impairment of IGHMPB2 transcript degradation. The treatment of SHSY-5Y neuroblastoma cells and control iPSCs with cycloheximide (CHX), which indirectly inhibits NMD by blocking translation, induced an increase of IGHMBP2 mRNA levels suggesting NMD regulation of IGHMBP2 transcript (online supplemental figure 5C).

We observed an increase in the abundance of a set of NMD target genes in SMARD1 MNs (figure 1E) and iPSCs (online supplemental figure 6A) compared with controls. Remarkably, the NMD-activating compound tranilast significatively decreased IGHMBP2 expression in SMARD1 MNs (figure 1G), and iPSCs (online supplemental figure 5D) and rescued the mRNA accumulation of some NMD targets both in MNs (figure 1F) and in iPSCs (online supplemental figure 6B). Importantly, NMD reactivation was also able to significantly rescue pathological MN hallmarks (figure 1H1). Moreover, in control iPSCs, NMD inhibition by CHX induced a variable increase in NMD-sensitive transcript isoforms (hnRNPL and TRA2B), which was less steep in SMARD1 iPSCs (online supplemental figure 7).

DISCUSSION

SMARD1 is a rare but fatal disease with onset in early childhood. It affects the lower MNs, causing distal limb paralysis and respiratory distress. In the present study, we described eight new SMARD1 cases and reported updated data for two previously described cases. Given the rarity of this disease, this represents a substantial cohort of SMARD1 patients. Our results confirmed reduced expression of full-length IGHMBP2 protein (to<5%) in all cell types. In cases involving nonsense mutations, IGHMBP2 was absent, whereas the protein was mildly reduced in the presence of a missense mutation.

We also demonstrated that very low IGHMBP2 protein generally predicts a severe phenotype. However, SMARD1 patients did not have significantly reduced IGHMBP2 mRNA levels, confirming previous findings.[1] We demonstrated that IGHMPB2 mRNA is regulated by NMD, a mechanism that eliminates mRNAs containing premature translation–termination codons, but also regulates the expression of a large number of genes and that NMD is impaired in SMARD1. Several mRNAs that are normally target of NMD were upregulated in SMARD1 iPSCs and MNs, and these changes were rescued by NMD pathway reactivation. Thus, NMD is emerging as a critical regulator of neuronal development, MN viability and axon growth. Insufficient NMD may indeed underlie neurodegeneration, such as in ALS.[3 5] Therefore, it is conceivable that NMD deficiency represents a pathogenic mechanism for SMARD1, causing accumulation of aberrant defective mRNA to which MNs are particularly sensitive. NMD rescue can reestablish the mRNA balance in MNs improving their pathological phenotype. Importantly, reactivation of the NMD pathway was able to rescue axon length and apoptosis in affected MNs, supporting the NMD pathway as a potential target, as previously suggested for other MN disorders.[3] Therefore, further investigations of drugs that can rescue NMD activity for potential therapeutic use in inherited motor neuropathies that share the same pathological molecular mechanism are warranted.

METHODS

Cell culture

Human samples were reprogrammed into iPSCs using the CytoTune-iPS V.2.0 Sendai Reprogramming Kit (Life Technologies). Spinal MNs were then obtained following a rapid multistage protocol.

The iPSCs and/or MNs were used in standard western blot analysis, and underwent immunohistochemistry for anti-human IGHMBP2 (Millipore) and

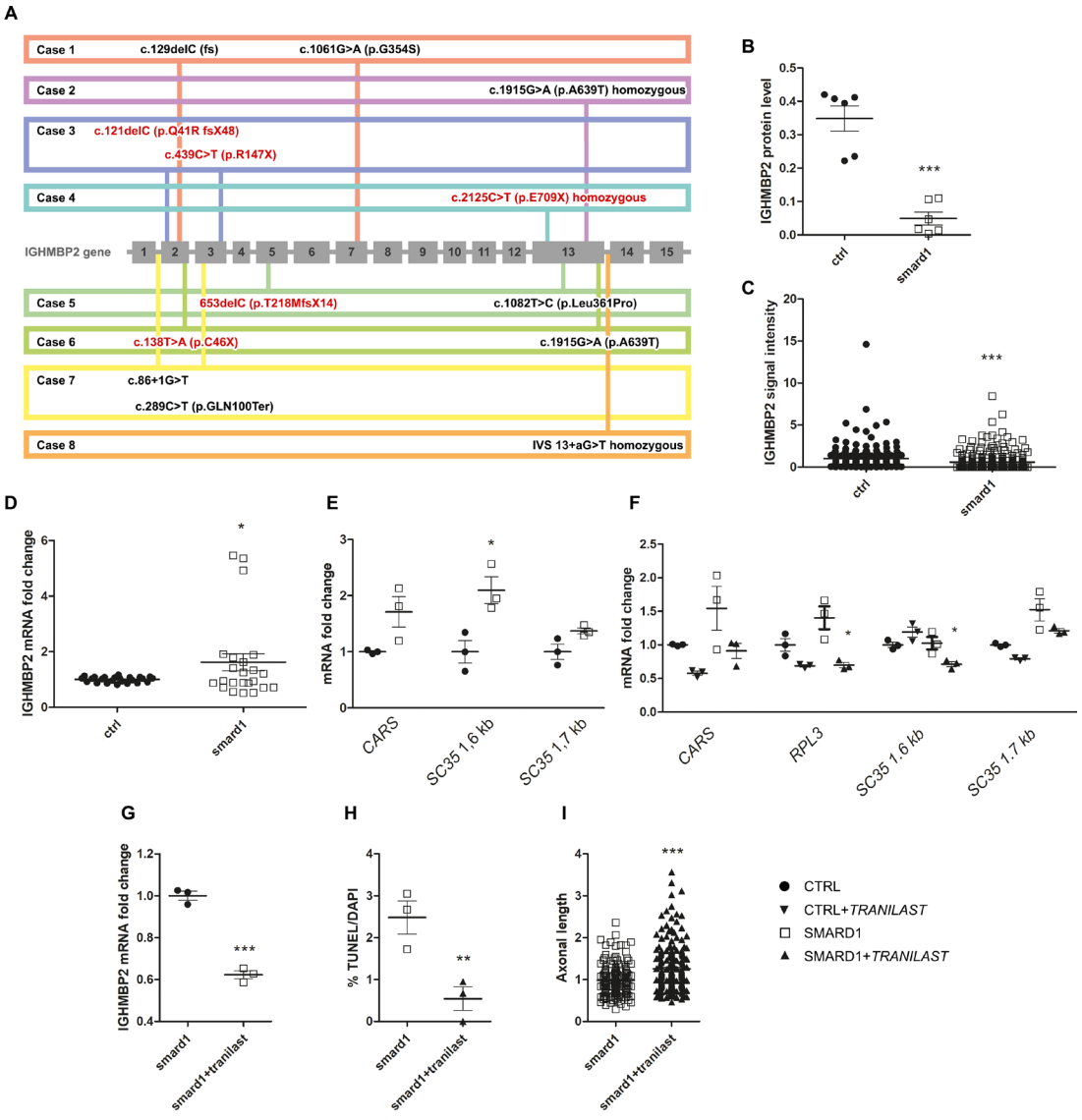

Figure 1 IGHMBP2 levels and nonsense-mediated mRNA decay (NMD) decay in hiPSC-derived motor neurons (MNs). (A) Schematic representation of the distribution along the immunoglobulin μ-binding protein 2 (IGHMBP2) gene of mutations found in the patient cohort. STOP codon mutations are indicated in red. (B) 110 kDa IGHMBP2 protein, assessed by western blot, decrease in spinal muscular atrophy with respiratory distress type I (SMARD1) MNs versus ctrl (***p<0.001, Student's t-test). (C) Immunocytochemistry quantification confirmed lower levels of IGHMBP2 in affected MNs ***p<0.001, *p<0.05, Student's t-test, ctrl versus patients (smard1, case 2, 3 and 6). (D) qPCR analyses of IGHMBP2 mRNA levels in affected MNs showed no correlation with protein level reduction, increasing in SMARD1 lines,*p<0.05, Student's t-test, ctrl versus patients. (E) mRNA levels of NMD target genes were increased in SMARD1 MNs versus ctrl (**p<0.01, Student's t-test). (F) RNA levels of NMD target genes were decreased after tranilast treatment in SMARD1 MNs (smard1, case 2, 3 and 6) versus ctrl (*p<0.05, Student's t-test). (G) mRNA levels of IGHMBP2 were rescued after treatment with tranilast (5 μM) in SMARD1 MNs, ***p<0.001, Student's t-test. (H,I) Treatment with the activator of NMD tranilast (5 μM) rescued pathological hallmarks of SMARD1 MNs (smard1, case 2, 3 and 6), namely apoptosis evaluated by tunel assay (E, **p<0.01, Student's t-test) and axon length reduction (F, ***p<0.001, Student's t-test). In B, E–H, each data point represents the mean obtained from three technical replicates for each biological replicate (n=3, smard1: case 2, 3 and 6). In D, each data point represents a technical replicate (biological replicates n=3 for ctrl, n=4 for smard1, case 2, 3, 6 and 7). In C and I, each point represents data from a single cell. Values are presented±SEM. All the images are original and made by the authors.

SMI-32 (Millipore) and the terminal deoxynucleotidyl transferase dUTP nick end labelling system protocol (Promega). IGHMBP2 expression was evaluated by standard TaqMan qPCR assay. For transcripts known to be regulated by NMD, SYBR Green Real Time PCR was used.

The iPSCs and/or MNs were treated with transcription inhibitor actinomycin D at 2.5 μg/mL, with 100 μg/mL CHX for 6 hour and 5 μM tranilast (T0318-10MG) for 24 hours.

Michela Taiana,[1] Alessandra Govoni,[2] Sabrina Salani,[2] Nicole Kleinschmidt,[3] Noemi Galli,[2] Matteo Saladini,[1] Stefano Bruno Ghezzi,[2] Valentina Melzi,[2] Margherita Bersani,[1] Roberto Del Bo,[1] Oliver Muehlemann,[3] Enrico Bertini,[4] Valeria Sansone,[5,6] Emilio Albamonte,[6] Sonia Messina,[7,8] Francesco Mari,[9] Elisabetta Cesaroni,[10] Liliana Porfiri,[10] Francesco Danilo Tiziano,[11] Gian Luca Vita,[7] Maria Sframeli,[7] Carmen Bonanno,[8] Nereo Bresolin,[1,2] Giacomo Comi,[1,2,12] Stefania Corti ,[1,2] Monica Nizzardo [2]

[1]Dino Ferrari Centre, Neuroscience Section, Department of Pathophysiology and Transplantation (DEPT), University of Milan, Milano, Lombardia, Italy
[2]Neurology Unit, Fondazione IRCCS Ca' Granda Ospedale Maggiore Policlinico, Milan, Lombardia, Italy

[3]Department of Chemistry and Biochemistry, University of Bern, Bern, Switzerland
[4]Department of Neuroscience, Unit of Neuromuscolar and Neurodegenerative Diseases, IRCCS Bambino Gesù Children's Hospital, Rome, Italy
[5]Department Biomedical Sciences for Health, University of Milan, Milano, Lombardia, Italy
[6]NEuroMuscular Omnicentre (NEMO), ASST Grande Ospedale Metropolitano Niguarda, Fondazione Serena Onlus, Milan, Italy
[7]NEMO SUD Clinical Centre for Neuromuscular Disorders, Messina, Italy
[8]Department of Clinical and Experimental Medicine, University of Messina, Messina, Italy
[9]Child Neurology Unit, Pediatric Hospital A. Meyer, Florence, Italy
[10]Department of Child Neuropsychiatry, Children's Hospital G. Salesi -University of Ancona, Ancona, Italy
[11]Institute of Genomic Medicine, Università Cattolica del Sacro Cuore Fondazione, Policlinico Universitario Agostino Gemelli, Roma, Lazio, Italy
[12]Neuromuscular and rare diseases unit, Fondazione IRCCS Ca' Granda Ospedale Maggiore Policlinico, Milan, Lombardia, Italy

Correspondence to Dr Monica Nizzardo, IRCCS Foundation Maggiore Policlinico Hospital, Milan, Lombardia, Italy; monica.nizzardo1@gmail.com

Acknowledgements The authors wish to thank Associazione Amici del Centro Dino Ferrari for its support.

Contributors MT and AG contributed equally to this paper. MN and SC contributed equally to this paper. MN and SC conceived the presented idea. MT and MN planned the experiments. MT carried out in vitro the experiment with the support of NG and MB. SS performed western blot analysis. SBG and VM. performed qPCR experiments. RDB performed genetic analysis on mutations. GPC and NB helped supervise the project. MC and MN wrote the manuscript with support from MS and AG. AG, EB, VAS, EA, SM, FM, EC, LP, DT, GLV, MS, CB provide sample and clinical information on patients and healthy subjects. SC and MN conceived and planned the experiments.

Funding This study was supported by Cariplo Foundation (to MN, 2015-0776), Research and Innovation Staff Exchange CROSS-NEUROD Grant ID: 778 003 to SC and Italian Ministery of Health Foundation IRCCS Ca' Granda Ospedale Maggiore Policlinico Ricerca Corrente 2020 to GPC and NB.

Competing interests None declared.

Patient consent for publication Not applicable.

Ethics approval This study involves human participants and was approved by Institutional Ethical Committee 0004520 Participants gave informed consent to participate in the study before taking part. This study was conducted in accordance with the Code of Ethics of the World Medical Association (Declaration of Helsinki) and its later amendments, and with national legislation and institutional guidelines.

Provenance and peer review Not commissioned; externally peer reviewed.

► Additional supplemental material is published online only. To view, please visit the journal online (http://dx.doi.org/10.1136/jnnp-2021-326425).

To cite Taiana M, Govoni A, Salani S, *et al*. *J Neurol Neurosurg Psychiatry* 2022;**93**:908–910.

Received 17 February 2021
Accepted 17 December 2021
Published Online First 27 January 2022

J Neurol Neurosurg Psychiatry 2022;**93**:908–910. doi:10.1136/jnnp-2021-326425

ORCID iDs
Stefania Corti http://orcid.org/0000-0001-5425-969X
Monica Nizzardo http://orcid.org/0000-0001-5447-0882

REFERENCES

1 Saladini M, Nizzardo M, Govoni A, *et al*. Spinal muscular atrophy with respiratory distress type 1: clinical phenotypes, molecular pathogenesis and therapeutic insights. *J Cell Mol Med* 2020;24:1169–78.
2 Dehecq M, Decourty L, Namane A, *et al*. Nonsense-Mediated mRNA decay involves two distinct Upf1-bound complexes. *Embo J* 2018;37:e99278.
3 Xu W, Bao P, Jiang X, *et al*. Reactivation of nonsense-mediated mRNA decay protects against C9orf72 dipeptide-repeat neurotoxicity. *Brain* 2019;142:1349–64.
4 Grohmann K, Rossoll W, Kobsar I, *et al*. Characterization of Ighmbp2 in motor neurons and implications for the pathomechanism in a mouse model of human spinal muscular atrophy with respiratory distress type 1 (SMARD1). *Hum Mol Genet* 2004;13:2031–42.
5 Jaffrey SR, Wilkinson MF. Nonsense-mediated RNA decay in the brain: emerging modulator of neural development and disease. *Nat Rev Neurosci* 2018;19:715–28.

Supplementary material

Molecular analysis of SMARD1 patient-derived cells demonstrates that nonsense-mediated mRNA decay is impaired

Michela Taiana[1]*, Alessandra Govoni[2]*, Sabrina Salani[2], Nicole Kleinschmidt[3], Noemi Galli[1], Matteo Saladini[1], Stefano Bruno Ghezzi[2], Margherita Bersani[1], Valentina Melzi[2], Roberto Del Bo[1], Oliver Mühlemann[3], Enrico Bertini[4], Valeria A Sansone[5,6], Emilio Albamonte[5], Sonia Messina[7,8], Francesco Mari[9], Elisabetta Cesaroni[10], Liliana Porfiri[10], Danilo Tiziano[11], Gian Luca Vita[8], Maria Sframeli[8], Carmen Bonanno[7], Nereo Bresolin[1,2], Giacomo P. Comi[1,2,12], Stefania Corti[1,2]°, and Monica Nizzardo[2]°**

1 Dino Ferrari Centre, Neuroscience Section, Department of Pathophysiology and Transplantation (DEPT), University of Milan

2 Foundation IRCCS Ca' Granda Ospedale Maggiore Policlinico, Neurology Unit, Milan, Italy.

3 Department of Chemistry and Biochemistry, University of Bern, CH-3012 Bern, Switzerland

4 Department of Neuroscience - Unit of Neuromuscolar and Neurodegenerative Diseases, IRCCS Bambino Gesù Children's Hospital, Rome, Italy.

5 NEuroMuscular Omnicentre (NEMO), ASST Grande Ospedale Metropolitano Niguarda, Fondazione Serena Onlus, Piazza Ospedale Maggiore, 3, 20162, Milan, Italy.

6 Department Biomedical Sciences for Health, Università degli Studi di Milano, Milan, Italy

7 Department of Clinical and Experimental Medicine, University of Messina, Messina, Italy

8 NEMO SUD Clinical Centre for Neuromuscular Disorders, Messina, Italy

9 Child Neurology Unit, Pediatric Hospital “A. Meyer”, Viale Pieraccini 24, Florence, Italy

10 Department of Child Neuropsychiatry,G. Salesi Children's Hospital-University of Ancona, Ancona, Italy.

11 Institute of Genomic Medicine, Università Cattolica del Sacro Cuore Fondazione, Policlinico Universitario Agostino Gemelli IRCCS, Rome, Italy

12 Foundation IRCCS Ca’ Granda Ospedale Maggiore Policlinico, Neuromuscular and rare diseases unit, Milan, Italy.

**Corresponding author: Neuroscience Section, Department of Pathophysiology and Transplantation (DEPT), University of Milan, Neurology Unit, IRCCS Foundation Ca’ Granda Ospedale Maggiore Policlinico, Via Francesco Sforza 35, 20122 Milan Italy. Tel: +39 0255033833; Fax: +39 0255033800; Email: monica.nizzardo1@gmail.com, ORCID ID: 0000-0001-5447-0882

Supplementary Figure 1

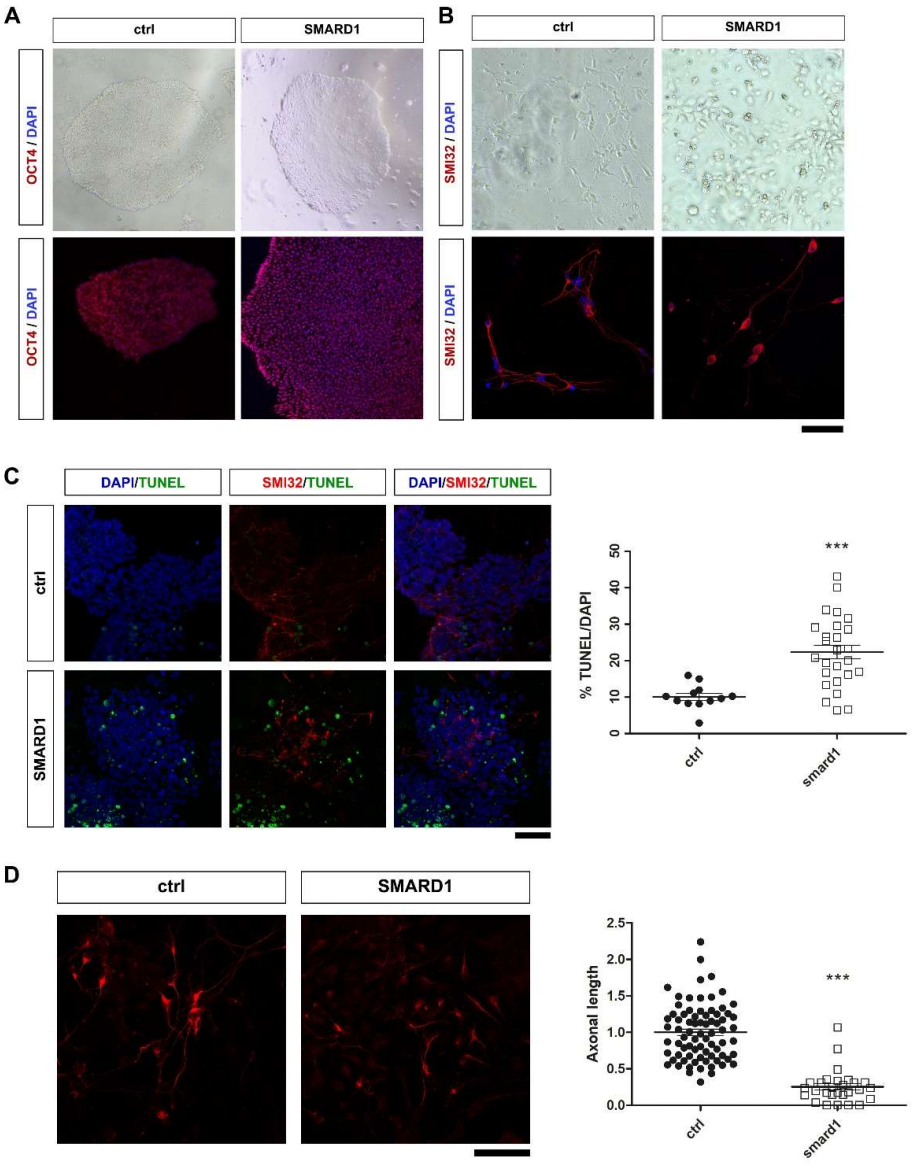

iPSCs and MNs generation

(A, B) Representative image of (A) the three controls (ctrl) and the four SMARD1 iPSCs colonies (brightfield upper panel) expressing specific pluripotent marker (lower panel, OCT4, red) and (B) MNs positive for MN marker (SMI32) from control (n = 3) and SMARD1 (n = 3) cases. Nuclei are

labelled with DAPI (blue). (C, D) Representative images of controls (ctrl) and SMARD1 MNs. DNA fragmentation Tunel assay showed an increased apoptosis (Tunel green, SMI32 red, DAPI, blue, **p* < 0.01, Student's t-test, n = 3 biological replicates) in SMARD1 cases. Each data point represents 1 technical replicate. (C). Quantification of MN axon length revealed a decrease in smard1 in respect with ctrl (****p* < 0.001, Student's t-test). Each point represents data from a single cell. Values are presented as means ± SEM. Scale bar: 100µm for (A, C) and 50 µm for (B, C).

Supplementary Figure 2

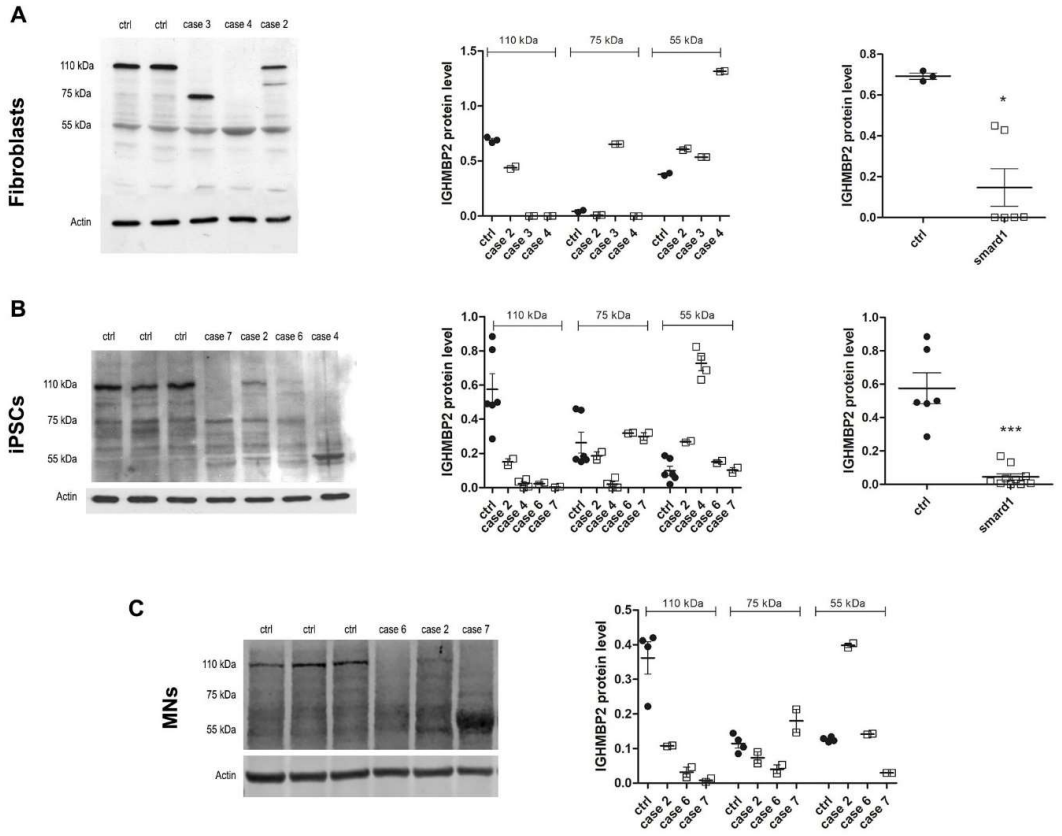

Full-length IGHMBP2 protein is decreased in SMARD1 patient cell lines

IGHMBP2 protein level was assessed by western blot in fibroblasts (A), iPSCs (B) and MNs (C) from patients and controls. Three different IGHMBP2 isoforms were detected at 110 kDa (full length), 75 kDa, and 55 kDa. The 110-kDa form was decreased in all SMARD1 samples, and expression of truncated forms (75 kDa and 55 kDa) varied by case. First column: representative image of western blot; second column: quantification of the protein level for each case, each data point represents 1 technical replicate; third column: quantification of the 110-kDa protein pooled for controls (ctrl) and patients (smard1). *$p < 0.05$ for fibroblasts, and ***$p < 0.001$ for iPSCs, Student's t-test. Values are presented ± SEM.

Supplementary Figure 3

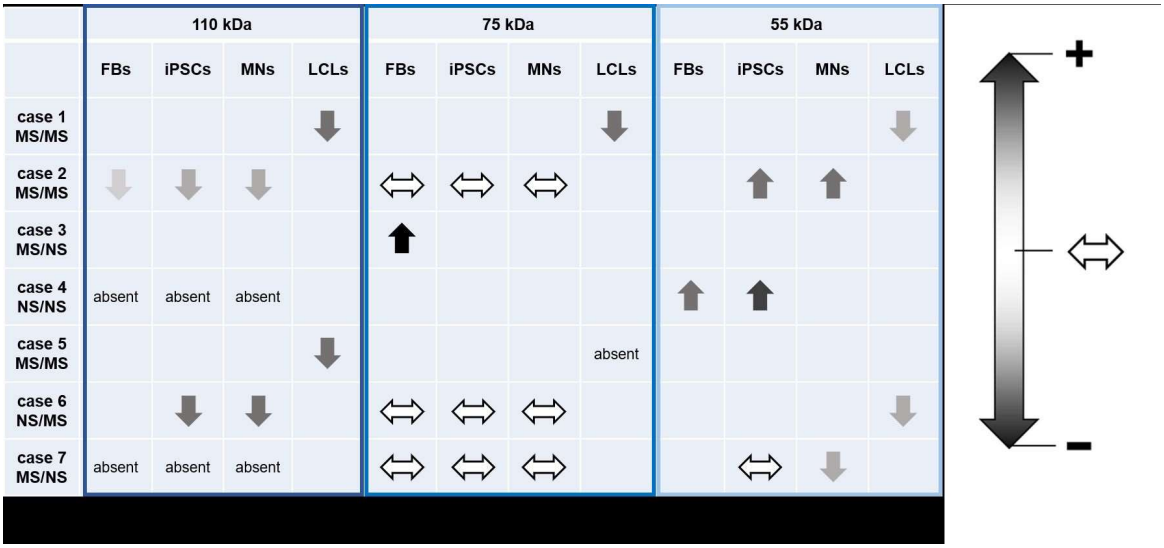

Schematic representation of the different IGHMBP2 protein expression levels

Schematic representation of the different IGHMBP2 protein expression levels relative to control in SMARD1 fibroblasts (FBs), iPSCs, and MNs assessed by western blot (110-kDa, 75-kDa, and 55-kDa bands). Horizontal arrows indicate unvaried protein levels, up arrows indicated increased levels, and down arrows indicate decreased levels compared to control. Greyscale shows the percentage of variation compared to control, from unvaried (white) to highest variation (black). Absent indicates undetectable protein. MS: missense, NS: nonsense.

Supplementary Figure 4

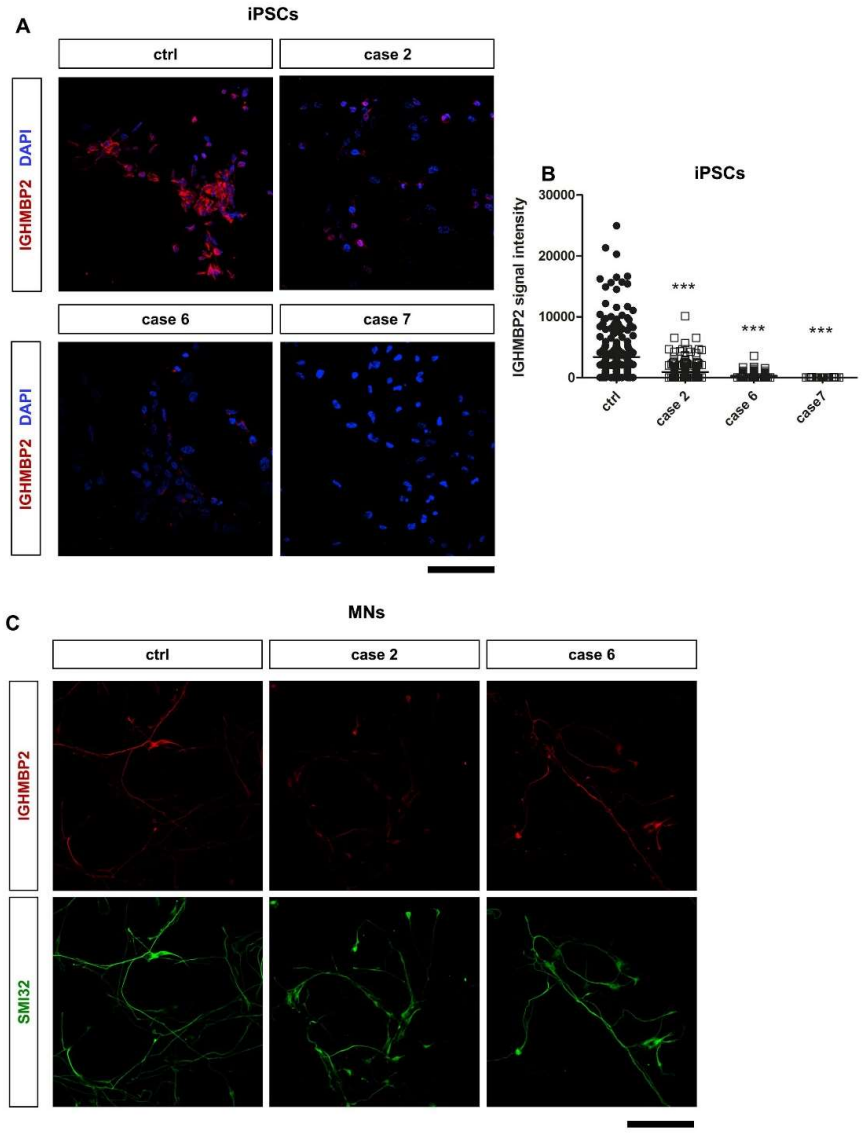

IGHMBP2 protein is decreased in SMARD1 iPSC-derived lines

Representative images of immunocytochemistry of iPSCs (A, DAPI in blue) and iPSC-derived MNs (C, SMI32 in green) obtained from patients with SMARD1. iPSCs showed a decrease in IGHMBP2 protein expression (red) compared to controls (ctrl). Graphs represent the immunoreactivity score quantified using ImageJ software of IGHMBP2 in iPSCs (B), n=3 technical replicates; 4 fields imaged and analyzed per replicate. Each data point represents a single cell, ***$p < 0.001$, Student's t-test, ctrl vs single case. Values are presented ± SEM.s. Scale bar: 75 µm for iPSCs and 50 µm for MNs.

Supplementary Figure 5

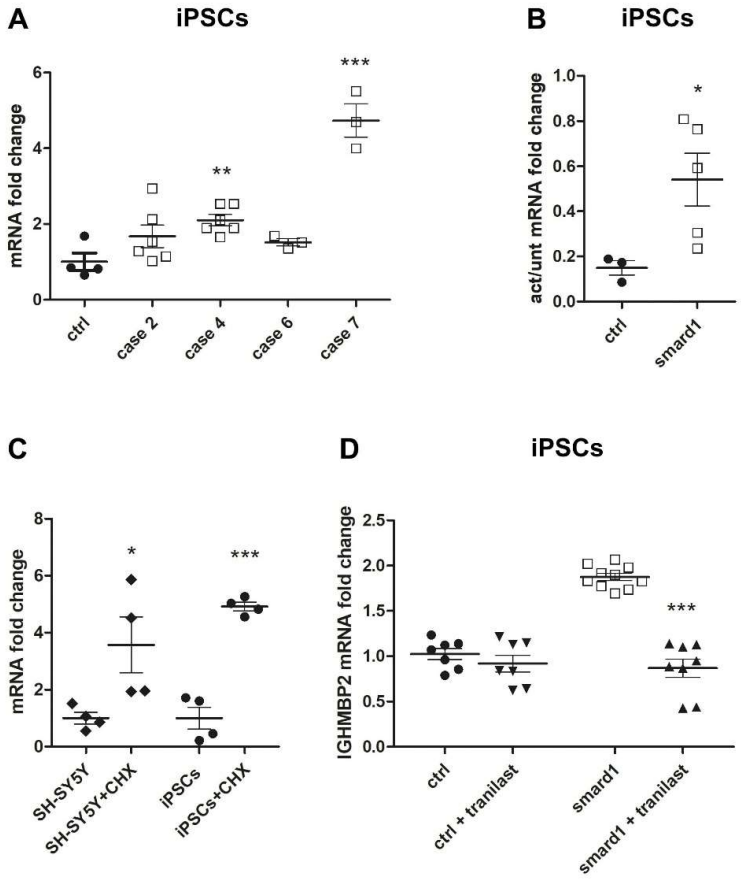

***IGHMBP2* degradation is impaired in SMARD1-derived cell lines and regulated by NMD**

qPCR analyses of *IGHMBP2* mRNA levels in iPSCs (A) showed no correlation with protein level reduction in SMARD1 cell lines and were increased compared to control (ctrl, n = 3) in specific SMARD1 cases, each data point represents a single technical replicate (**p < 0.01, ***p < 0.001, Student's t-test, ctrl vs single case). (B) Evaluation of *IGHMBP2* mRNA half-life after actinomycin D 2.5 µg/ml (act)-induced transcription inhibition revealed increased mRNA stabilization in SMARD1 iPSCs (cases 2, 6, and 7) compared to controls (n = 3), suggesting impairment of *IGHMBP2* mRNA decay, each data point represents the mean of 3 technical replicates (***p < 0.001, Student's t-test). (C) qPCR evaluation of *IGHMBP2* expression after NMD inhibition by 100 µg/ml CHX for 6 h showed a significant increase in mRNA levels compared to basal expression of untreated

cells in the neuronal cell line SHSY-5Y and in control iPSCs, suggesting NMD-mediated degradation of *IGHMBP2* mRNA, each data point represents 1 technical replicate. (*p < 0.05, ***p < 0.001, Student's t-test). (D) *IGHMBP2* mRNA level decreased in SMARD1 iPSCs after the treatment with tranilast (5 μM), an activator of NMD. n=3 biological replicates, each data point represents a single technical replicate (***p < 0.001, Student's t-test), further supporting the hypothesis that *IGHMBP2* mRNA is a target for NMD. Values are presented ± SEM.

Supplementary Figure 6

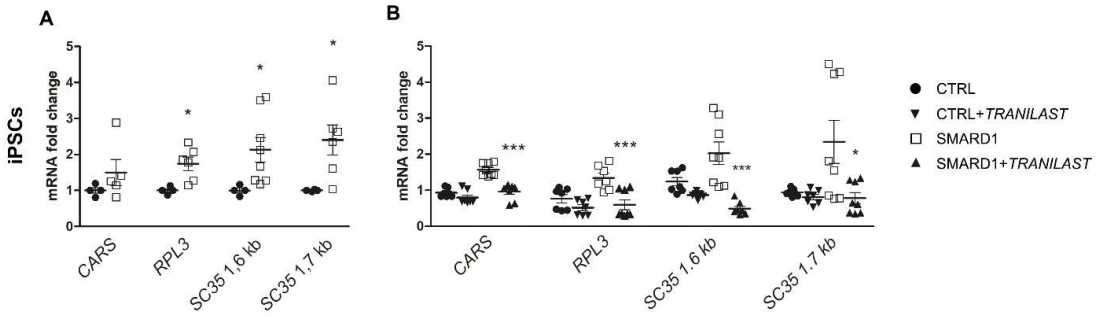

NMD is impaired in SMARD1-derived cell lines

(A) mRNA levels of NMD target genes were increased in SMARD1 iPSCs (cases 2, 6, and 7) compared to controls (*$p < 0.05$, Student's t-test); (B) mRNA levels of NMD target genes were rescued after treatment with tranilast (5 μM) in SMARD1 iPSCs (cases 2, 6, and 7, *$p < 0.05$, ***$p < 0.001$, Student's t-test, each data point represents a single technical replicate); Values are presented ± SEM at least from three independent experiments.

Supplementary Figure 7

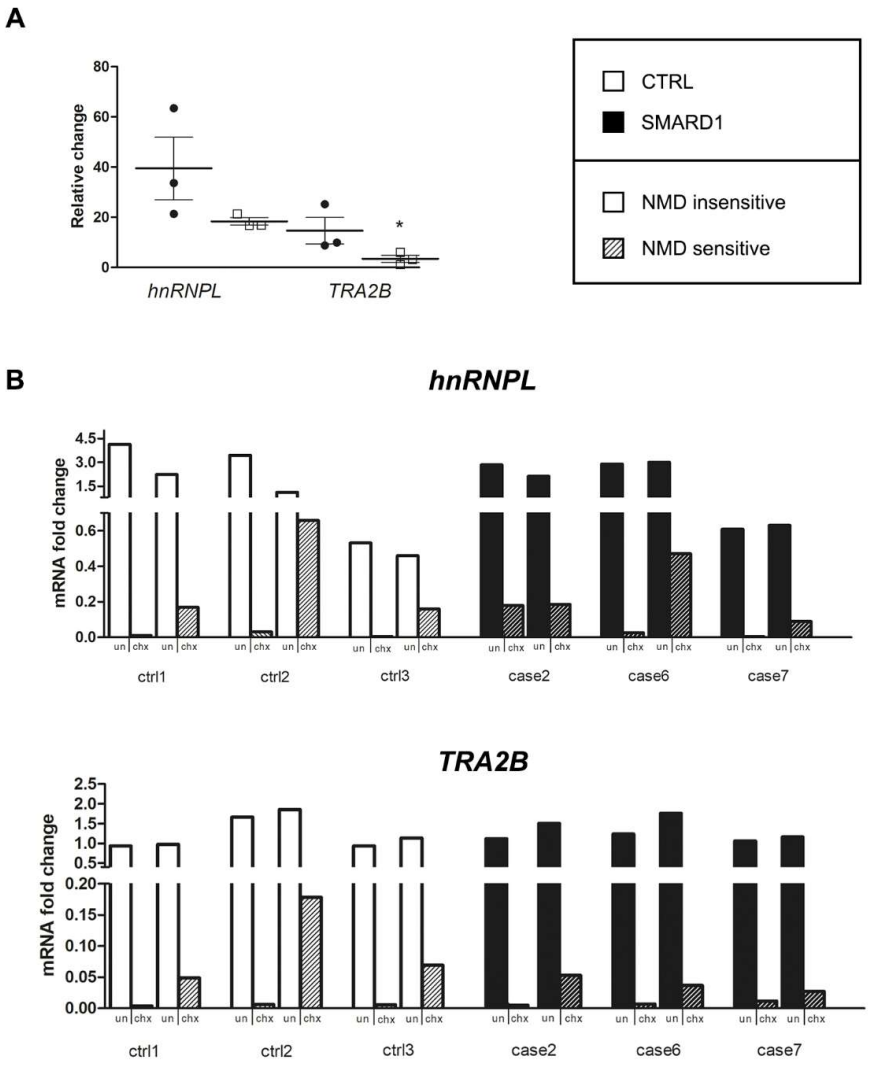

NMD efficacy impaired in SMARD1 patients' iPSCs

(A)Assessment of a relative increase in the NMD-sensitive isoform normalized to the NMD-insensitive isoform level of *hnRNPL* and *TRA2B* after NMD inhibition showed a reduction in NMD activity in SMARD1 iPSCs (cases 2, 6, and 7) compared to control. The ratio between $2^{-\Delta CT}$ NMD-sens/ $2^{-\Delta CT}$ NMD-ins isoforms was calculated for each sample, and its relative change after CHX treatment ((CHX-unt)/unt) was evaluated for each cell line. Each data point represents the mean of 3

technical replicate (*$p < 0.05$, Student's t-test). (B) mRNA fold change of (A) separate for each cell lines (cases 2, 6, and 7). Notably, different cases and controls presented high mRNA levels variability.

Supplementary Table 1

Patient (gender)	Age at onset	Motor milestone achieved	Ventilation	G-tube	Current motor ability	Mutations	Position	Reference
Case 1 (M)	≤ 3 months	sitting position	tracheostomy	not now, only temporarily	tetra-paresis, minimal movements of proximal upper limbs	c.1061G>A (p.G354S)	ex 7	[21]
						c.129delC (fs)	ex 2	
Case 2 (M)	≤ 3 months	none	tracheostomy	yes	tetra-paresis, minimal movements of proximal upper limbs	c.1915G>A (p.A639T) homozygous	ex 13	novel
Case 3 (F)	≤ 3 months	poor neck control	tracheostomy	yes	tetra-paresis, antigravity movements minimally preserved at upper limbs	c.121delC (p.Q41R fsX48)	ex 2	novel
						c.439C>T (p.R147X)	ex 3	NM_002180.2 (IGHMBP2): c.439C>T (p.R147T)
Case 4 (F)	> 3 months	none	tracheostomy	yes	/	c.2125C>T (p.E709X) homozygous	ex 13	novel
Case 5 (F)	≤ 3 months	none	/	no	/	653delC (p.T218MfsX14)	ex 5	novel
						1082T>C (p.L361P)	ex 13	NM_002180.2 (IGHMBP2): c.1082T>C (p.L361P)
Case 6 (F)	> 3 months	Crawling at six months, standing position at 1 year	continuous NIV, cough assistance	yes	tetra-paresis, minimal movements of proximal upper limbs, social interactions and language skills appropriate for the age, evident tendon retraction at wrists, hip joints and ankles	c.138T>A (p.C46X)	ex 2	[11]
						c.1915G>A (p.A639T)	ex 13	novel
Case 7 (M)	≤ 3 months	none	tracheostomy	yes	tetra-paresis, minimal movements of proximal upper limbs, can communicate only by his facial mimics and eye movements	c. 86+1G>T	int 1	novel
						c. 289C>T (p.Q100X)	ex 3	novel
Case 8 (F)	> 3 months	independent sitting by 14 months and ability to walk with support by 27 months	continuous NIV	yes	tetra-paresis, minimal movements of proximal upper limbs, severe rotoscoliosis	IVS 13+1G>T homozygous	/	[21]

Clinical and genetic characteristics of the patients' cohort. Right column: mutation references.

Supplementary Table 2

Characteristics of healthy donors (controls)

	gender	age at the sample collection
ctrl 1	male	at birth
ctrl 2	male	7 years
ctrl 3	male	19 years

Supplementary methods

Genetic sequencing

Blood samples from the patients were processed for the extraction of DNA. The 15 coding exons and flanking intronic regions of the *IGHMBP2* gene (NM_002180.2) were amplified by PCR, using the TaqMan Universal PCR Master Mix solution (Applied Biosystems). The amplification was performed using forward and reverse primers (Invitrogen) for each exon, as described in a previous study [1]. All PCR products were sequenced using the BigDye Terminator 3.1 protocol on an ABI-Prism 3130 Genetic Analyzer (Applied Biosystems). We conducted the sequence alignment and analysis with SeqScape software (Applied Biosystem).

iPSC generation and differentiation

From the blood and skin biopsy specimens of patients and controls, we obtained lymphoblastoid (cases 1 and 5) and fibroblast (cases 2, 3, 4, 6, 7, 8) cells and cultured them as previously described.[41] The fibroblasts of cases 2, 4, 6 and 7 were then reprogrammed with a non-integrating viral protocol using the CytoTune®-iPS 2.0 Sendai Reprogramming Kit (Life Technologies). Spinal MNs were then obtained from wild-type and SMARD1 iPSCs following a rapid (14-days) multistage protocol that has been previously described [2].

Western blot analyses

The cells were sonicated and centrifuged at 13,500 rpm for 10 min at 4°C. A total of 20 µg of each sample was separated using 12% SDS-PAGE and then transferred to a nitrocellulose membrane, saturated with 1% bovine serum albumin, 10% horse serum, and 0.075% Tween 20 in TBS (20 mM Tris-HCl, 0.5 M NaCl) solution for 1 h. The membrane was then incubated overnight at 4°C with the primary antibody (anti-human IGHMBP2 (1:800, Millipore) or anti-α-actin (1:250, Sigma) as loading control) in saturating solution. After 24 h, the membrane was incubated with a secondary horseradish peroxidase–conjugated antibody (Molecular Probes/Invitrogen) in saturating solution. The western

blot bands were detected via enhanced chemiluminescence (Amersham). Densitometric analysis was performed using Image J software.

Immunocytochemistry

Cells were fixed on coverslips in 4% paraformaldehyde, permeabilized in 0.25% Triton X-100, and blocked in 10% bovine serum albumin and 0.3% Triton X-100 in 1x PBS solution for 1 h at room temperature. After an incubation overnight with antibodies (anti-human IGHMBP2, Millipore, 1:500 dilution; SMI-32, Millipore, 1:100 dilution), cells were incubated with a 1:2000 anti-mouse immunoglobulin G Alexa Fluor 488-A11008 secondary antibody (Invitrogen) for 1 h. Detection of apoptotic cells was carried out using the terminal deoxynucleotidyl transferase dUTP nick end labelling (TUNEL) system protocol (Promega). For quantification four random fields for each sample were acquired and TUNEL positive cells were counted on the total of DAPI positive nuclei. Axonal length, detected as SMI-32–positive prolongation, was assessed considering only the longest projection completely included in the acquired field for each MN. Quantification has been performed selecting 10 random fields for each sample as previously described [3]. Quantification analysis was performed using Image J software.

Transcript analysis

RNA extraction was performed on iPSCs and MNs derived from patients and controls, using the ReliaPrep™ RNA Cell Miniprep System kit (Promega) following the manufacturer's instructions, and dosed with NanoDrop One (ThermoFisher Scientific). Reverse-transcribed material (20 ng for each well) was amplified in triplicate using the TaqMan Universal PCR Master Mix (Applied Biosystems) and appropriate probe to evaluate *IGHMBP2* gene expression (Hs01045548_m1) by means of the ΔΔCt method on a 7500 Real Time PCR System (Software 2.01, Applied Biosystems). Expression levels were normalized to the average level of the housekeeping gene 18S (Hs99999901_s1) and referred to the relevant control samples.

With the same conditions, a qPCR analysis to quantify RNA was then performed for other transcripts known to be regulated by NMD [4], using the SYBR Green Real Time PCR Master Mix. The forward and reverse primers used were as follows: *IGHMBP2* NM-002180.2, FW 5'-GAAGACCCTGGTGGAGTATTT-3' and RW 5'-CTGGAAGTTCTCATGGGAATAG-3'); *IGHMBP2* XM-005273976.1, FW 5'-CTGCTGAAGGCCAGAAAG-3' and RW 5'-CCAGGGATGTGTCTACAGATTG-3'); *RPL3*, FW 5'-GGCATTGTGGGCTACGTG-3' and RW 5'-CTTCAGGAGCAGAGCAGA-3'); *CARS*, FW 5'-AAATTAAATGAGACCACGGA-3' and RW 5'-TGACATCACAGCCAAGTGTA-3'); *SC35 1.6kb*, FW 5'-CGGTGTCCTCTTAAGAAAATGATGTA-3' and RW 5'-CTGCTACACAACTGCGCCTTTT-3'; and *SC35 1.7kb*, FW 5'-GGCGTGTATTGGAGCAGATGTA-3' and RW 5'-CTGCTACACAACTGCGCCTTTT-3'. We also determined the relative RNA levels of the endogenous NMD-sensitive transcripts *HNRNPL_NMD* and *TRA2B_NMD* and their corresponding NMD-insensitive splice forms *HNRNPL_PROT* and *TRA2B_PROT*. For this purpose, 16 ng of the reverse-transcribed total RNA was amplified in triplicate using Brilliant III Ultra-Fast SYBR® Green QPCR Master Mix (Agilent) and the following primer pairs: *HNRNPL_NMD*, FW 5'-GGTCGCAGTGTATGTTTGATG-3' and RW 5'-GGCGTTTGTTGGGGTTGCT-3'; TRA2B_NMD, FW 5'-TGGAATCAGAAAGCACTACGC-3' and RW 5'-GAATCTTCCTTGGAGCGAGA-3'; *HNRNPL_PROT*, FW 5'-CAATCTCAGTGGACAAGGTG-3' and RW 5'-CTCCATATTCTGCGGGGTGA-3'; and *TRA2B_PROT*, FW 5'-GAGGTTGGCAGCTTCGATT-3' and RW 5'-AAGCAGAACGGGATTCCC-3'. Expression levels were normalized to the average level of *β-actin* (*ACTB*) as internal control FW 5'-ACGGCTCCGGCATGTGCAAG-3' and RW TGACGATGCCGTGCTCGATG.

References

[1] Grohmann K, Schuelke M, Diers A, Hoffmann K, Lucke B, Adams C et al (2001) Mutations in the gene encoding immunoglobulin mu-binding protein 2 cause spinal muscular atrophy with respiratory distress type 1. Nat Genet 29:75-77.

[2] Maury Y, Côme J, Piskorowski RA, Salah-Mohellibi N et al (2015) Combinatorial analysis of developmental cues efficiently converts human pluripotent stem cells into multiple neuronal subtypes. Nat Biotechnol 33(1):89-96.

[3] Nizzardo M, Simone C, Rizzo F, Salani S, Dametti S, Rinchetti P et al (2015) Gene therapy rescues disease phenotype in a spinal muscular atrophy with respiratory distress type 1 (SMARD1) mouse model. Sci Adv 1(2):e1500078.

[4] Linde L, Boelz S, Neu-Yilik G, Kulozik AE, Kerem B (2007) The efficiency of nonsense-mediated mRNA decay is an inherent character and varies among different cells. Eur J Hum Genet 15(11):1156-62.